Single grain TT-OSL ages for the Earlier Stone Age site of Bestwood 1 (Northern Cape Province, South Africa)

Maïlys Richard, Michael Chazan, Naomi Porat

Single grain TT-OSL ages for the Earlier Stone Age site of Bestwood 1 (Northern Cape Province, South Africa)

Richard M.[1, 2]*, Chazan M.[3,4], Porat N.[2]

[1]Centre de Recherche Français à Jérusalem, 3 Shimshon Street, Jerusalem, Israel
[2]Geological Survey of Israel, 32 Yesha'yahu Leibowitz, Jerusalem, Israel
[3]Department of Anthropology, University of Toronto, 19 Russell St, Toronto, Canada
[4]Institute of Evolutionary Studies, University of the Witwatersrand, Johannesburg, South Africa

*Corresponding author: mailys.richard@lsce.ipsl.fr
Current address: Laboratoire des Sciences du Climat et de l'Environnement, LSCE/IPSL, UMR CEA-CNRS-UVSQ 8212, Université Paris-Saclay, Gif sur Yvette, France.

Abstract

The transition from the Earlier Stone Age (ESA) to the Middle Stone Age (MSA) in the interior of southern Africa is associated with the Fauresmith Industry. Major cultural developments found in the Fauresmith include regular use of ochre and other coloured minerals, prepared core technology including blade and point production, and the use of hafted spears. Chronological control for the Fauresmith is weak so that critical questions regarding the relationship of this industry to the evolution of modern humans remain unresolved. Here we present ages for the Bestwood 1 site, an open-air locality in the Northern Cape Province (South Africa) where an extensive Fauresmith occupation is found underlying sand deposits.

Optically stimulated luminescence (OSL) was first applied to samples from the sands overlying the Bestwood 1 occupation horizon, and from the occupation horizon itself, in order to establish the chronology of the site. However, sediment mixing resulting from bioturbation processes has been observed, causing post-depositional bleaching of the majority of the grains, thus limiting the use of OSL. In addition, given the identification of the lithic assemblage to the Fauresmith, it seems likely that the sands were beyond the dating range of conventional OSL. Due to its hard-to-bleach properties, the thermally transferred-optically

stimulated luminescence (TT-OSL) signal was deemed suitable for detecting the least-bleached grains.

Single grain TT-OSL analyses combined with the finite mixture model (FMM) were conducted in order to isolate the oldest grains that could be contemporaneous with the time of deposition of the sediment associated with the ESA assemblage. High scattering of the equivalent doses is consistent with bioturbation processes that mixed sediment; the distribution of the equivalent dose values suggests that younger grains were incorporated into the ESA layers, thus supporting the use of the oldest component determined using the FMM to calculate the TT-OSL ages. This approach allowed us to establish the time for the Fauresmith occupation at 366 ± 32 ka, and the age of the overlying sand deposits, spanning from 350 ± 22 ka to 226 ± 13 ka.

Key-words: Earlier Stone Age; Fauresmith; Chronology; Luminescence; TT-OSL; Bioturbation; Finite Mixture Model

1. Introduction

Luminescence dating has played a critical role in the archaeology of early modern humans in Africa and the Middle East, and Neanderthals in Europe and the Middle East. Optically stimulated luminescence (OSL) and thermoluminescence (TL) provide widely applicable means of chronological control for periods as far back as 300 ka. For earlier sites, there is a very real challenge in correlating the timing of the archaeological record with the stages of hominin evolution leading up to the emergence of modern humans. In southern Africa, the immediate challenge is to establish the chronology of the Fauresmith industry, which represents the local transition between the Earlier Stone Age and the Middle Stone Age (Chazan 2015a, see Herries 2011; see Underhill 2011 for critical discussion of the Fauresmith). At Kathu Pan 1, the Fauresmith Stratum 4a is dated by OSL of quartz to 464 ± 47 ka and by U-series/ESR of tooth enamel to 542 +140/-107 ka (Porat et al. 2010). The Kathu Pan 1 archaeological assemblage is notable for the presence of ochre and specularite, the use of a prepared core method of flake, point and blade production, and evidence for the use of points as hafted spears (Wilkins et al., 2012; Watts et al., 2016). At Canteen Kopje, Finite Mixture Model (FMM) OSL ages obtained for the base of the section, overlying the

Fauresmith layer, ranged from 164 ± 9 ka (CK7-6) to 167 ± 10 ka (CK7-5) (Chazan et al. 2013).

The site of Bestwood 1 (Northern Cape Province, South Africa, Fig. 1) is an extensive locality situated in a north-facing valley between two hills on the western flank of the Kuruman Hills (Chazan et al. 2012, Papadimitrios et al. 2019). Lithic material was first identified at the edges of a sand quarry, leading to excavations at areas designated Block 1 (29 m²) and Block 2 (16 m²) at the southern end of the quarry. In both Block 1 and 2 a continuous distribution of artefacts in fresh (unabraded) condition were found across the entire excavation area lying on the top of a gravel deposit (with a thickness >20 m.) and below clean sands. Similar sections were found in test pits excavated 250 and 800 m to the north. There is a typological consistency across these excavation areas, with a combination of bifaces and prepared core technology. Bestwood 1 thus represents an extensive hominin occupation across a landscape which, based on Ground Penetrating Radar survey, is reconstructed as the banks of a small stream (Papadimitrios et al., 2019).

For Middle Pleistocene deposits, the development of extended-range luminescence methods, such as thermally transferred optically stimulated luminescence (TT-OSL), allowed the dating of quartz beyond the limits of conventional OSL. TT-OSL is based on the transfer of charge from deeper traps to the main OSL traps, induced after depleting the OSL signal and preheating the sample to high temperature (i.e., 260°C). The TT-OSL signal was observed in early luminescence dating studies (e.g., Aitken and Smith, 1988; Rhodes, 1988) but its use for dating was proposed in 2006 (Wang et al., 2006a; Wang et al., 2006b). Two components have been identified in the TT-OSL signal, named the Recuperated OSL (ReOSL) and the Basic Transferred OSL (BT-OSL) (Aitken, 1998). The ReOSL is the signal used to construct the dose response curve (DRC) and to obtain the equivalent dose (D_e) in TT-OSL dating studies; the BT-OSL is a residual signal that remains after depletion of the ReOSL signal. Single aliquot regeneration (SAR) protocols were thus proposed to isolate the BT-OSL (e.g., Wang et al., 2007; Tsukamoto et al., 2008). However, a study led by Kim et al. (2009) suggests that the BT-OSL signal contribution to the TT-OSL signal might be negligible and that its subtraction does not impact significantly the DRC nor the D_e. A simplified protocol, which does not involve a separate measurement of the BT-OSL signal but includes a depletion of this component using heat treatment at 300°C at the end of the SAR cycle, was proposed by Porat et al. (2009), and a modified protocol (after Adamiec et al., 2010) was applied in this study.

The reliability of TT-OSL dating has been tested in a number of studies by comparing results with independent or semi-independent dating methods, especially at the Atapuerca sites in Spain (e.g., Arnold et al., 2015; Demuro et al., 2019). The sensitivity of the TT-OSL signal to light exposure is much lower than the conventional OSL signal, resulting in slow optical resetting rate (Porat et al., 2009; Jacobs et al., 2011). Indeed, only well-bleached samples can be considered for TT-OSL, since bleaching experiments have shown that exposure to daylight prior to deposition must be in the order of several weeks or months to reset the signal and avoid age overestimation (Fig. 4 in Jacobs et al., 2011).

However, based on the assumption that the TT-OSL signal bleaches much slower than the OSL signal, this property can be used in environments where bioturbation is predominant and has been constant over time, limiting the use of conventional OSL. This is the case of the open-air site of Bestwood 1. Preliminary OSL measurements revealed a high scatter in the D_e distribution, whether using single or multi-grain analyses (SOM Tab. S1). Moreover, the obtained ages were far too young for the industries found at the site. It is assumed that intense bioturbation processes are responsible for this scatter. Indeed, ants and termites can cause vertical and lateral displacement of grains, and favour the incorporation of bleached grains originating from the top of the sequence, whose signal has been reset (e.g., Bateman et al., 2007; Rink et al., 2013).

The use of single grain (SG) measurements can provide information on the dose distribution, especially in environments where differential bleaching and sediment mixing is expected. As the TT-OSL signal is bleached much slower than the OSL signal by several orders of magnitude, we hypothesized that for some grains the signal might not have been bleached during the intense bioturbation; these grains could be isolated by SG TT-OSL measurements. This innovative application of SG TT-OSL, combined with the use of the Finite Mixture Model (FMM, Galbraith and Green, 1990), allows to isolate the oldest grain component, avoiding the bleached grains in the samples. This approach is fundamental in establishing the chronology of Bestwood 1.

2. Material and method

Samples for luminescence dating were collected from the main section in the sand unit (samples BSW-5 and 6), at the boundary between the sand and gravel units (BSW-7), and in

the gravel unit (BSW-8) in the excavated square, by hammering light-proof PVC pipes into the section (Fig. 2).

2.1. Sample preparation

Sample preparation and all measurements were conducted at the Geological Survey of Israel according to the procedure detailed in Faershtein et al. (2016). Wet sieving was performed to extract the most abundant grain size, 125-150 μm. Quartz grains were purified with 8% HCl to dissolve carbonates, followed by magnetic separation to remove heavy minerals and most feldspars. The remaining feldspars were dissolved and the quartz etched to eliminate the alpha dose component using 40% HF for 40 minutes, followed by overnight soaking in 16% HCl to dissolve any fluorides which may have precipitated.

2.2. Equivalent dose determination

OSL analyses were first conducted on 2 mm aliquots using a modified single aliquot regenerative (SAR) protocol (Murray and Wintle, 2000) (SOM Tab. S2). Dose recovery tests over a range of preheats showed that a recovery dose ratio of 0.99 ± 0.05 can be obtained using a preheat of 10 s at 260ºC, a test dose of ~9.3 Gy with a preheat of 5 s at 200 ºC. All samples show good recycling ratios within 10% of 1.0 and negligible IR signals. However, high overdispersion (OD) values and relatively young OSL ages (SOM Tab. S1) are consistent with bioturbated sands. SG measurements of one sample further highlighted the severe mixed and bleached character of the sample, giving an age of 60 ± 50 ka (SOM Tab. S1). To isolate the oldest dose component, SG TT-OSL measurements were undertaken following the SAR protocol of Porat et al. (2009), including a thermal bleach (310°C for 100 s) at the end of each cycle to remove the contribution from the BT-OSL component (Tab. 1). Single-grain disks with 300 μm holes were loaded with 125-150 μm quartz grains. Using a binocular microscope, it has been observed that up to three or four grains filled each hole, thus increasing the yield compared to ideal SG measurements (Arnold et al., 2014; Arnold et al., 2015). Indeed, the yield of grains accepted according to our selection criteria is high, ranging from 12% to 20% (Tab. 2).

Equivalent doses were determined on a TL/OSL DA-20 Risø reader (Bøtter-Jensen and Murray, 1999). A green laser was used for stimulation and the signal was detected with a 7.5-mm U-340 filter. Aliquots were irradiated using the inbuilt $^{90}Sr/^{90}Y$ beta-source with dose

159 rate to the SG disc of 0.049 $Gy \cdot s^{-1}$. The TT-OSL signal was normalised using the subsequent
160 OSL signal measured after delivering a test dose of ~25 Gy (Porat et al., 2009).

161 The data were processed using Analyst v.4.57 (Duller, 2007). The signal was
162 integrated using the first 0.125 s and background was subtracted from the last 0.25 s. The
163 following criteria were applied for D_e selection: a recycling ratio limit of 1 ± 0.25;
164 recuperation < 20% of the natural signal; maximum test dose error of 30%; and a test dose
165 signal > 3 sigma above background. Equivalent doses were obtained using an exponential
166 fitting function. The statistical treatment of the D_e values was done using the Finite Mixture
167 Model (FMM, Galbraith and Green, 1990) using a sigma-b value of 0.15 based on single
168 grain measurements of the well-bleached Risø calibration quartz (OD = 11-22%), a good
169 analogue for the measured sands. However, instead of using the most frequent grain
170 population (e.g., Chazan et al., 2013), ages were calculated from the highest D_e population,
171 with the condition that this component represents at least 10% of the overall grains. This
172 threshold was selected so that the oldest component is not biased by very few outlying grains,
173 (e.g. Rodnight et al., 2005) and it is considered reasonable taking into account the number of
174 viable grains (> 100 grains).

175 **2.3. Dose rate determination**

176 Water content was estimated at 5 ± 3%, due to the sandy and loose nature of the
177 sediment. Alpha, beta and gamma dose rates were derived from the radioactive content
178 measured by inductively coupled plasma-mass spectrometry (ICP-MS) for uranium and
179 thorium and inductively coupled plasma optical emission spectrometry (ICP-OES) for
180 potassium, using the conversion factors of Guérin et al. (2011). Uncertainties of 3% (K), 5%
181 (U) and 10% (Th) were derived from comparison to international standards and repeated
182 measurements. Cosmic dose rates were estimated from current burial depths according to the
183 equations of Prescott and Hutton (1988).

184

185 **3. Results**

186 The TT-OSL signals are mostly bright, and the DRC's are sub-linear (Fig. 3). The
187 chosen data processing results in ages in stratigraphic order. Dose rates, equivalent doses and
188 SG TT-OSL ages are presented in Tab. 2 and SOM Tab. S1. The alpha, beta and gamma dose
189 rates derived from U, Th and K contents are homogeneous within the sand unit, resulting in

dose rates that range from 0.58 to 0.67 Gy/ka for samples BSW-5 to 7 (Tab. 2 and SOM Tab. 1). Sample BSW-8 was collected from the gravel layers, for which the dose rate is slightly higher (0.73 Gy/ka). Sampling depths ranges from 1.9 to 2.3 m, and even at such depths the corresponding cosmic dose rate is significant, representing between 18% and 22% of the total dose rate.

Since bioturbation processes have been observed along the sequence, the use of the Central Age Model (Galbraith et al., 1999) is not appropriate. Indeed, the broad range of D_e values (Fig. 4), the indistinguishable CAM ages along the sequence, and the high OD values that range from 54 to 63% (SOM Tab. 1) even without the rejected "zero-age" grains, (SOM Tab. 1) are consistent with the mixing of sediment by post-depositional processes. Instead of using the Maximum Age Model, which is sensitive to anomalously high outliers, the Finite Mixture Model (Galbraith and Green, 1990) was applied to isolate the significant D_e components, using the BIC criterion (Galbraith and Roberts, 2012), and selecting the oldest component that comprises more than 10% of the grains (see e.g. Rodnight et al., 2005 for a similar selection criterion when choosing the youngest De component). Three components were identified for each sample (Fig. 4 and SOM Tab. S3). The highest D_e component represents the oldest grain population, assuming that for these grains the TT-OSL signal has been least bleached during post-depositional processes. These De values are based on 11 to 42% of the grains (Tab. 2). The presence in all samples of "zero-age" grains that their TT-OSL signal has been well bleached, indicates that bioturbation is an on-going process. These grains did not pass the selection criteria and have a natural TT-OSL intensity close to 0, but TT-OSL signals can be generated and a DRC constructed (Fig. 3A), providing D_e values close to 0 Gy (< 5 Gy). The "zero-age" grains raise the possibility that even the oldest grain component might underestimate the true age of the site because these grains could have been exposed to sunlight and partially bleached. The cumulative light sum curves obtained are similar for the four samples (Fig. 5). As for such curves obtained for SG OSL data (e.g. Duller et al., 2000), the light distribution among the grains is not equal, meaning that a small number of grains dominate the signal in multi-grains measurements.

Additionally, to assess the level of bleaching of the TT-OSL signal in such environments, measurements were conducted on three Holocene samples from the neighboring site of Kathu Pan (SOM Tab. S4), situated about 5 km away from Bestwood and also constructed of sandy sediments (Lukich et al., 2020). These samples yielded low OSL D_e (≤ 2 Gy) (Lukich et al., 2019; 2020). The TT-OSL signal was measured on three aliquots from

each sample, a total of 9 D_e determinations. Eight out of the nine aliquots were well bleached, with TT-OSL D_e values ranging from 4.7-18 Gy, and an average of 9.9 ± 4.5 Gy (SOM Tab. S4). This value is similar to the lowest value measured in "modern" samples by Duller and Wintle (2012) and can be considered as the minimum residual. In addition to the "zero-age" grains, these measurements support our assumption that the TT-OSL signal was well bleached at the time the quartz grains were initially deposited at the site, but they also raise concerns that even the oldest TT-OSL grains might have been exposed to some sunlight and partially bleached. Hence the ages should be considered as minimum.

The ages obtained using the highest D_e component are (from bottom to top; Tab. 2) 366 ± 32 ka for the gravel layer (BSW-8), and 350 ± 22 ka (BSW-7), 295 ± 17 ka (BSW-6) and 226 ± 13 ka (BSW-5) for the sand unit. These ages are in stratigraphic order and the one obtained for the gravel layer, 366 ± 32 ka, provides a minimum age for the living surface where artefacts were discovered.

4. Discussion

4.1. Bioturbation processes and the use of single grain TT-OSL to extract the oldest component

Bioturbation has been reported in similar contexts at other sites, limiting the use of optical dating of the sediment: the presence of different age populations among the dated grains affects the accuracy of the ages and limits their precision (e.g., Tribolo et al., 2010), in particular in unconsolidated sands (e.g., Schoville et al., 2009; Chazan et al., 2013; Kristensen et al., 2015; Williams, 2019). Indeed, the lack of any sedimentary structures in the sands at Bestwood indicates that bioturbation occurred. Nonetheless, the use of the FMM allows to extract the oldest component, i.e. to discard younger grains that were likely bleached after deposition.

The transportation of grains by ants or termites can lead to different scenarios, for example, the introduction of younger grains from the top of the section through galleries or the transportation of older grains from the lower levels to the surface by termites to construct their mounds. Kristensen et al. (2015) studied the effect of termites bioturbation on the OSL De values distribution and identified a few saturated grains in the upper 100 cm in termite mounds in a savannah ecosystem in Ghana, interpreted as an occasional loss of grains by the termites on the way to the surface. This is also suggested by Rink et al. (2013) for ants

activity. The authors also show that downward movement of grains occured from the surface to the depth, through galleries. The grain displacement may also occur laterally, representing a major issue for the application of luminescence dating (e.g., Bateman et al., 2007; Rink et al., 2013; Kristensen et al., 2015). On the one hand, these processes can lead to age underestimation, when grains are transported downwards from the surface with their signal reset. On the other hand, ages can also be overestimated appear when grains are brought upward in the section but not to the surface (no zeroing), as evidenced by Rink et al. (2013), and defined as "subterranean-transported".

However, in the case of Bestwood 1, the majority of the grains dated using both conventional OSL and TT-OSL were considered to be too young according to the archaeological context of the deposit.Taking into account the minimum-maximum OSL or TT-OSL age ranges and the average ages for each of the dated samples (SOM Table S1), the young SG component clearly impacts the average D_e values. It suggests that the introduction down-section of zeroed grains was the main consequence of bioturbation processes and that any averaging would cause age underestimation for these samples; only the use of the FMM to isolate the oldest component could circumvent age underestimations. In addition, the presence of zero-age grains suggests that bioturbation is an ongoing process. That there are also TT-OSL zero-age grains deep in the section gives an insight into the thorough resetting of the quartz TT-OSL signal. Lastly, the SG TT-OSL ages calculated using the oldest component are in stratigraphic order and in agreement with the archaeological record, supporting the use of SG TT-OSL combined with the FMM to calculate ages for bioturbated sandy deposits.

4.2. Significance of the ages

The chronology of the Fauresmith industry is, to date, not well defined. Similarly bioturbated sediments at Canteen Kopje produced a Fauresmith industry but the use of OSL dating was limited by sediment mixing (Chazan et al., 2013). At Canteen Kopje, the Fauresmith was found right above the gravel (McNabb and Beaumont, 2011; Lotter et al., 2016). Single-grain (micro-aliquot) OSL ages obtained for the base of the sandy section that overlies the gravel unit can thus give a minimum age for the Fauresmith. Chazan et al. (2013) used the FMM to select the largest SG population, and obtained ages of 167 ± 10 ka (CK7-5) and of 164 ± 9 ka (CK7-6) for the lowermost samples. Following our approach to isolate the

oldest grain component and avoid the bleached grains in these samples, a re-analyses of the SG OSL data from Chazan et al. (2013) gave ages of 307 ± 24 ka (CK7-5) and 292 ± 17 ka (CK7-6). They are somewhat younger than the SG TT-OSL FMM ages obtained for Bestwood 1, but they can be considered as minimum ages for the Fauresmith as they overly the layers where this industry was found.

Other published age determinations for the Fauresmith are U-Th ages from the sites of Rooidam and Wonderwerk Cave, which in both cases do not provide a conclusive age for the occupation. At Rooidam, there are two U-Th ages on calcrete from strata overlying Archaeological Stratum 9 (Unit B), which produced a rich archaeological assemblage attributed to the Fauresmith (Butzer, 1974). Samples BUT 2 from Unit C and BUT 1 from Unit G (two meters higher in the sequence) are dated to 108 ± 20 ka and 151 ± 35 ka, respectively (Szabo and Butzer, 1979). The younger age of BUT 2 appears to be the result of recrystallization of calcite. There is apparently a small assemblage also attributed to the Fauresmith from Unit F, which underlies BUT 1. Thus, the Rooidam data supports a chronology of the Fauresmith at greater than 150 kyr but does not provide an actual age for the assemblage.

Beaumont and Vogel (2006) have published several U-Th ages from three excavation areas in Wonderwerk Cave that are relevant to the age of the Fauresmith. From Excavations 6 at the back of the cave there is a single U-Th minimum age of 187 ± 8 ka on a speleothem (sample U576)). Although Beaumont and Vogel attribute the archaeological assemblage to the MSA, it is most likely Fauresmith based on current understanding of this assemblage (Chazan, 2015a). However, questions remain about the temporal relationship between this speleothem and the depositional context in which it was found (Herries, 2011). Beaumont and Vogel also report U-Th ages for Excavation 2 (U437 - 276 ± 29 ka; U499 - 278 ± 26 ka; U583 - 286 ± 29 ka) as coming from a Fauresmith context, however re-examination of the associated archaeological assemblages does not find adequate indications to confirm this cultural attribution. In Excavation 1, two speleothems from the top of the Acheulean sequence (U427, U407; Stratum 6) produced ages of >350 ka. Typologically the associated assemblage (Stratum 6) shows some characteristics that link it to the Fauresmith (Chazan, 2015).

Based on our TT-OSL data for Bestwood 1, on the reanalysed OSL data from Canteen Kopje and on published data from Kathu Pan, the Fauresmith industry is older than ~350 ka. The SG TT-OSL age obtained for the human occupation layer at Bestwood 1, of 366 ± 32 ka,

is in agreement with updated minimum ages for the industry at the base of the section at Canteen Kopje, of around 300 ka. The ages are however younger than those obtained for the Fauresmith industry at Kathu Pan, for which a minimum OSL age of 464 ± 47 ka and a combined U-series–ESR age of 542 +140/-107 were obtained (Porat et al., 2010).

5. Conclusion

Based on the observations that the TT-OSL signal bleaches much slower than the OSL signal, single grain TT-OSL analyses were conducted in order to isolate the oldest grains, i.e., the grains that were the least affected by bioturbation and surface exposure. The slow optical resetting rate of the TT-OSL signal is generally considered as an obstacle; nonetheless, bioturbated sediment can benefit from this property, allowing to discard the younger grain component whose signal has been partially reset during transportation and burrowing by ants and termites.

At Bestwood 1, this innovative application combined with the use of the FMM, allows to isolate the oldest component that is thought to be contemporaneous with the deposition time of the sediment associated to the ESA assemblage. The age obtained for the human occupation layer, of 366 ± 32 ka, allows to constrain human presence at the site during MIS 11-10. The chronology of the overlying sand deposits, spanning from 350 ± 22 ka to 226 ± 13 ka (MIS 10 to 8), suggest that the lower part of the stratigraphic section dated in this study was deposited in less than 150 ka.

The regional chronology suggests that the Fauresmith industry appeared around 500 ka, according to ESR and OSL ages obtained at Kathu Pan. Our data from Bestwood 1, as well as updated ages for Canteen Kopje, are consistent with such an early age but allow for a persistence of the Fauresmith to at least ~360 ka. These new data confirm the overlap between the timing of the Fauresmith and the first appearance of modern humans and predates the age of the Florisbad fossil (Grün et al., 1996; Richter et al., 2017). Our approach to isolate the oldest grains component, using single grain TT-OSL combined with FMM, opens new perspectives in dating bioturbated sediment.

Acknowledgments

This work was part of a postdoctoral fellowship granted to MR from the French Research Institute in Jerusalem (CRFJ). We thank Yael Jacobi-Glass for performing TT-OSL measurements on the Holocene samples from Kathu Pan. We thank the Social Sciences and Humanities Research Council of Canada and the Paleontological Scientific Trust. All fieldwork and export of samples under permit from the South African Heritage Resources Agency (SAHRA). Fieldwork on Block 1 was co-supervised by Steven James Walker. Thanks to the Cawood family for access to their farm and all their assistance. We thank the three anonymous reviewers for their constructive remarks on this manuscript.

References

Aitken, M.J., Smith, B.W., 1988. Optical dating: Recuperation after bleaching, Quaternary Science Reviews 7, 387-393.

Aitken, M.J., 1998. An Introduction to Optical Dating, Oxford Science Publications, Oxford.

Adamiec, G., Duller, G.A.T., Roberts, H.M., and Wintle, A.G., 2010. Improving the TT-OSL SAR protocol through source trap characterization, Radiation Measurements, 45, 768–777.

Arnold, L.J., Demuro, M., Parés, J.M., Arsuaga, J.L., Aranburu, A., Bermúdez de Castro, J.M., Carbonell, E., 2014. Luminescence dating and palaeomagnetic age constraint on hominins from Sima de los Huesos, Atapuerca, Spain, Journal of Human Evolution 67, 85-107.

Arnold, L.J., Demuro, M., Parés, J.M., Pérez-González, A., Arsuaga, J.L., Bermúdez de Castro, J.M., Carbonell, E., 2015. Evaluating the suitability of extended-range luminescence dating techniques over early and Middle Pleistocene timescales: Published datasets and case studies from Atapuerca, Spain, Quaternary International 389, 167-190.

Bateman, M.D., Boulter, C.H., Carr, A.S., Frederick, C.D., Peter, D., Wilder, M., 2007. Preserving the palaeoenvironmental record in Drylands: Bioturbation and its significance for luminescence-derived chronologies, Sedimentary Geology 195, 5-19.

Beaumont, P.B., Vogel, J.C., 2006. On a timescale for the past million years of human history in central South Africa, South African Journal of Science 102, 217–228.

Bøtter-Jensen, L., Murray, A.S., 1999. Developments in optically stimulated luminescence techniques for dating and retrospective dosimetry, Radiation protection dosimetry 84, 307-315.

382 Burow, C., Kreutzer, S., Dietze, M., Fuchs, M.C., Fischer, M., Schmidt, C., Brückner, H.,
383 2016. RLumShiny - A graphical user interface for the R Package 'Luminescence',
384 Ancient TL 34, 22-32.
385 Butzer, K.W., 1974. Geo-archeological interpretation of Acheulian calc-pan sites at
386 Doornlaagte and Rooidam (Kimberley, South Africa), Journal of Archaeological
387 Science 1, 1-25.
388 Chazan, M., 2015a. The Fauresmith and archaeological systematics, Changing climates,
389 ecosystems and environments within arid southern Africa and adjoining regions.
390 Palaeoecology of Africa 33, 59-70.
391 Chazan, M., 2015b. Technological Trends in the Acheulean of Wonderwerk Cave, South
392 Africa, African Archaeological Review 32, 701-728.
393 Chazan, M., Wilkins, J., Morris, D., Berna, F., 2012. Bestwood 1: a newly discovered Earlier
394 Stone Age living surface near Kathu, Northern Cape Province, South Africa, Antiquity
395 86.
396 Chazan, M., Porat, N., Sumner, T.A., Horwitz, L.K., 2013. The use of OSL dating in
397 unstructured sands: the archaeology and chronology of the Hutton Sands at Canteen
398 Kopje (Northern Cape Province, South Africa), Archaeological and Anthropological
399 Sciences 5, 351-363.
400 Demuro, M., Arnold, L.J., Aranburu, A., Gómez-Olivencia, A., Arsuaga, J.-L., 2019. Single-
401 grain OSL dating of the Middle Palaeolithic site of Galería de las Estatuas, Atapuerca
402 (Burgos, Spain), Quaternary Geochronology 49, 254-261.
403 Duller, G.A., 2007. Assessing the error on equivalent dose estimates derived from single
404 aliquot regenerative dose measurements, Ancient TL 25, 15-24.
405 Duller, G.A.T., Bøtter-Jensen, L., Murray, A.S., 2000. Optical dating of single sand-sized
406 grains of quartz: sources of variability, Radiation Measurements 32, 453-457.
407 Faershtein, G., Porat, N., Avni, Y., Matmon, A., 2016. Aggradation–incision transition in arid
408 environments at the end of the Pleistocene: An example from the Negev Highlands,
409 southern Israel, Geomorphology 253, 289-304.
410 Galbraith, R.F., Green, P.F., 1990. Estimating the component ages in a finite mixture,
411 International Journal of Radiation Applications and Instrumentation. Part D. Nuclear
412 Tracks and Radiation Measurements 17, 197-206.
413 Galbraith, R.F., Roberts, R.G., 2012. Statistical aspects of equivalent dose and error
414 calculation and display in OSL dating: An overview and some recommendations,
415 Quaternary Geochronology 11, 1-27.

Galbraith, R.F., Roberts, R.G., Laslett, G.M., Yoshida, H., Olley, J.M., 1999. Optical dating of single and multiple grains of quartz from Jinmium rock shelter, northern Australia: Part I, experimental design and statistical models, Archaeometry 41, 339-364.

Grün, R., Brink, J.S., Spooner, N.A., Taylor, L., Stringer, C.B., Franciscus, R.G., Murray, A.S., 1996. Direct dating of Florisbad hominid, Nature 382, 500-501.

Guérin, G., Mercier, N., Adamiec, G., 2011. Dose-rate conversion factors: update, Ancient TL 29, 5-8.

Herries, A.I., 2011. A chronological perspective on the Acheulian and its transition to the Middle Stone Age in southern Africa: the question of the Fauresmith, International Journal of Evolutionary Biology 2011.

Jacobs, Z., Roberts, R.G., Lachlan, T.J., Karkanas, P., Marean, C.W., Roberts, D.L., 2011. Development of the SAR TT-OSL procedure for dating Middle Pleistocene dune and shallow marine deposits along the southern Cape coast of South Africa, Quaternary Geochronology 6, 491-513.

Kim, J.C., Duller, G.A.T., Roberts, H.M., Wintle, A.G., Lee, Y.I., Yi, S.B., 2009. Dose dependence of thermally transferred optically stimulated luminescence signals in quartz, Radiation Measurements 44, 132-143.

Kristensen, J.A., Thomsen, K.J., Murray, A.S., Buylaert, J.-P., Jain, M., Breuning-Madsen, H., 2015. Quantification of termite bioturbation in a savannah ecosystem: Application of OSL dating, Quaternary Geochronology 30, 334-341.

Lotter, M.G., Gibbon, R.J., Kuman, K., Leader, G.M., Forssman, T., Granger, D.E., 2016. A geoarchaeological study of the middle and upper Pleistocene levels at Canteen Kopje, Northern Cape Province, South Africa, Geoarchaeology 31, 304-323.

Lukich, V., Porat, N., Faershtein, G., Cowling, S., Chazan, M., 2019. New Chronology and Stratigraphy for Kathu Pan 6, South Africa, Journal of Paleolithic Archaeology 2, 235-257.

Lukich, V., Cowling, S., Chazan, M., 2020. Palaeoenvironmental reconstruction of Kathu Pan, South Africa, based on sedimentological data, Quaternary Science Reviews 230, 106153.

McNabb, J., Beaumont, P., 2011. A report on the archaeological assemblages from excavations by Peter Beaumont at Canteen Koppie, Northern Cape, South Africa, Archaeopress, Oxford.

Murray, A.S., Wintle, A.G., 2000. Luminescence dating of quartz using an improved single-aliquot regenerative-dose protocol, Radiation Measurements 32, 57-73.

Papadimitrios, K.S., Bank, C.-G., Walker, S.J., Chazan, M., 2019. Palaeotopography of a Palaeolithic landscape at Bestwood 1, South Africa, from ground-penetrating radar and magnetometry, South African Journal of Science 115, 1-7.

Porat, N., Duller, G.A.T., Roberts, H.M., Wintle, A.G., 2009. A simplified SAR protocol for TT-OSL, Radiation Measurements 44, 538-542.

Porat, N., Chazan, M., Grün, R., Aubert, M., Eisenmann, V., Horwitz, L.K., 2010. New radiometric ages for the Fauresmith industry from Kathu Pan, southern Africa: Implications for the Earlier to Middle Stone Age transition, Journal of Archaeological Science 37, 269-283.

Prescott, J.R., Hutton, J.T., 1988. Cosmic ray and gamma ray dosimetry for TL and ESR, International Journal of Radiation Applications and Instrumentation. Part D. Nuclear Tracks and Radiation Measurements 14, 223-227.

Rhodes, E.J., 1988. Methodological considerations in the optical dating of quartz, Quaternary Science Reviews 7, 395-400.

Richter, D., Grün, R., Joannes-Boyau, R., Steele, T.E., Amani, F., Rué, M., Fernandes, P., Raynal, J.-P., Geraads, D., Ben-Ncer, A., Hublin, J.-J., McPherron, S.P., 2017. The age of the hominin fossils from Jebel Irhoud, Morocco, and the origins of the Middle Stone Age, Nature 546, 293.

Rink, W.J., Dunbar, J.S., Tschinkel, W.R., Kwapich, C., Repp, A., Stanton, W., Thulman, D.K., 2013. Subterranean transport and deposition of quartz by ants in sandy sites relevant to age overestimation in optical luminescence dating, Journal of Archaeological Science 40, 2217-2226.

Rodnight, H., Duller, G.A.T., Tooth, S., Wintle, A.G., 2005. Optical dating of a scroll-bar sequence on the Klip River, South Africa, to derive the lateral migration rate of a meander bend. The Holocene 15, 802–811.

Schoville, B.J., Burris, L.E., Todd, L.C., 2009. Experimental artifact transport by harvester ants (Pogonomyrmex sp.): Implications for patterns in the archaeological record, Journal of Taphonomy 7, 285-303.

Szabo, B.J., Butzer, K.W., 1979. Uranium-series dating of lacustrine limestones from pan deposits with final Acheulian assemblage at Rooidam, Kimberley district, South Africa, Quaternary Research 11, 257-260.

Tribolo, C., Mercier, N., Rasse, M., Soriano, S., Huysecom, E., 2010. Kobo 1 and L'Abri aux Vaches (Mali, West Africa): Two case studies for the optical dating of bioturbated sediments, Quaternary Geochronology 5, 317-323.

Tsukamoto, S., Duller, G.A.T., Wintle, A.G., 2008. Characteristics of thermally transferred optically stimulated luminescence (TT-OSL) in quartz and its potential for dating sediments, Radiation Measurements 43, 1204-1218.

Underhill, D., 2011. The study of the Fauresmith: A review, The South African Archaeological Bulletin, 15-26.

Wang, X.L., Lu, Y.C., Wintle, A.G., 2006a. Recuperated OSL dating of fine-grained quartz in Chinese loess, Quaternary Geochronology 1, 89-100.

Wang, X.L., Wintle, A.G., Lu, Y.C., 2006b. Thermally transferred luminescence in fine-grained quartz from Chinese loess: Basic observations, Radiation Measurements 41, 649-658.

Wang, X.L., Wintle, A.G., Lu, Y.C., 2007. Testing a single-aliquot protocol for recuperated OSL dating, Radiation Measurements 42, 380-391.

Watts, I., Chazan, M., Wilkins, J., 2016. Early evidence for brilliant ritualized display: Specularite use in the Northern Cape (South Africa) between~ 500 and~ 300 ka, Current Anthropology 57, 287-310.

Williams, M.A.J., 2019. Termites and stone lines - traps for the unwary archaeologist, Quaternary Science Reviews 226, 106028.

Wilkins, J., Schoville, B.J, Brown, K.S., Chazan M., 2012. Evidence for early hafted hunting technology, Science 338, 942-946.

Figures

Fig. 1. Location map of Bestwood 1 and other sites discussed in the text. Black squares: Modern towns and cities, OLF- Olifantshoek, KUR- Kuruman, KMB- Kimberley. Red circles: Archaeological sites, BW- Bestwood, KP- Kathu Pan, WW- Wonderwerk Cave, CK- Canteen Kopje, RD- Rooidam.

Fig. 2. The stratigraphic context of the OSL samples in relation to the archaeological horizon at Bestwood 1, Block 1. A: Profile in exposure of overlying sands with OSL samples BSW-1 to BSW-6. B: BSW-7. C: BSW-8. D: Stratigraphic column. E: Vertical projection facing west showing OSL samples and archaeological artefacts. Note the association of samples BSW-7 and BSW-8 with the archaeological horizon, which is flat and vertically constrained. Units in meters. F: Vertical projection facing south showing OSL samples and archaeological artefacts.

Fig. 3. Dose response curves for a “Zero-age” grain (A) and an old (B, 620 ± 40 Gy) grain from sample BSW-8.

Fig. 4. Abanico plots for all samples. The dash lines represent the mean value; the solid red lines the FMM components. Graphs produced using ‘RLumShiny’ (Burow et al., 2016).

Fig. 5. Cumulative light sum curves for all samples.


NAMIBIA
BOTSWANA
Johannesburg
SOUTH AFRICA
Cape Town
0 125 250 500
Km.
N
KUR
KP
BW
WW
OLF
Kuruman Hills
Ghaap Escarpment
Vaal River
CK
KMB
RD
0 50
Km.
N

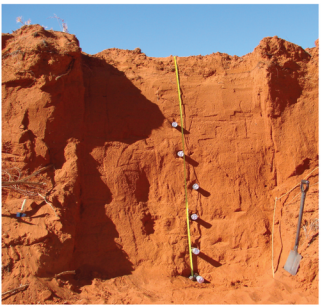

A

B

C


Compact sand with dispersed ironstone pea gravel
Ironstone gravel

D

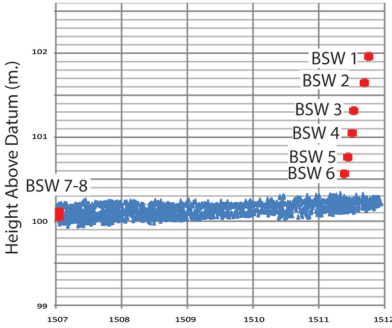
Height Above Datum (m.)
102
101
100
99
BSW 1
BSW 2
BSW 3
BSW 4
BSW 5
BSW 6
BSW 7-8
1507
1508
1509
1510
1511
1512
North South Grid Lines (m.)

E

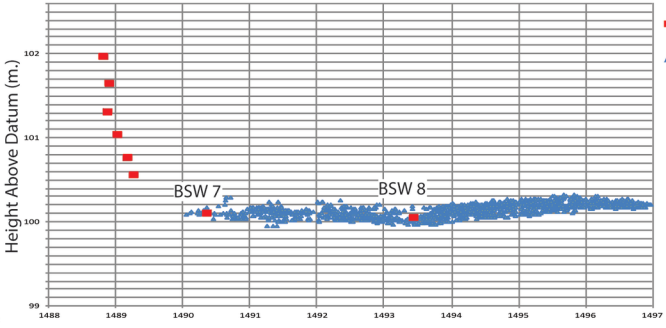
Height Above Datum (m.)
102
101
100
99
BSW 7
BSW 8
1488
1489
1490
1491
1492
1493
1494
1495
1496
1497
East West Grid Lines (m.)
OSL Sample
Artifact

F

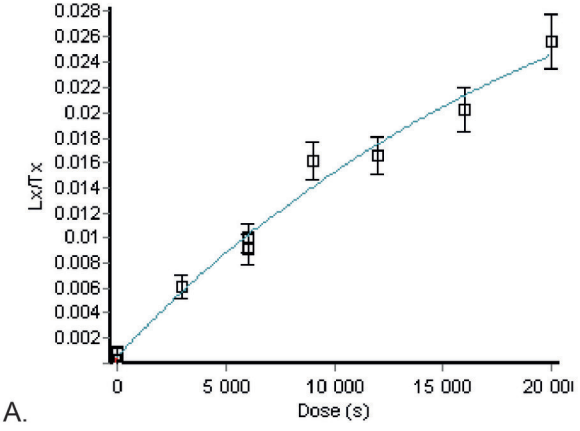
0.028
0.026
0.024
0.022
0.02
0.018
0.016
0.014
0.012
0.01
0.008
0.006
0.004
0.002
Lx/Tx
0
5 000
10 000
15 000
20 000
Dose (s)

A.

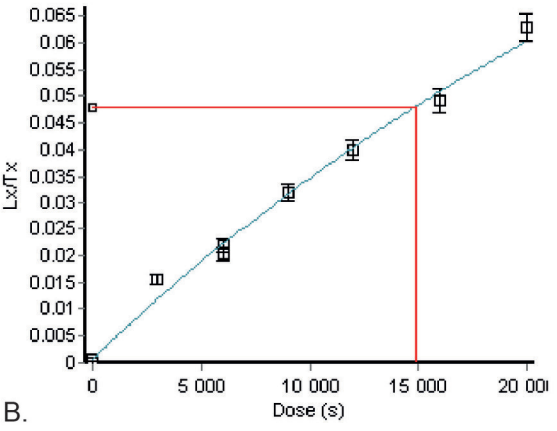
0.065
0.06
0.055
0.05
0.045
0.04
0.035
0.03
0.025
0.02
0.015
0.01
0.005
0
Lx/Tx
0
5 000
10 000
15 000
20 000
Dose (s)

B.

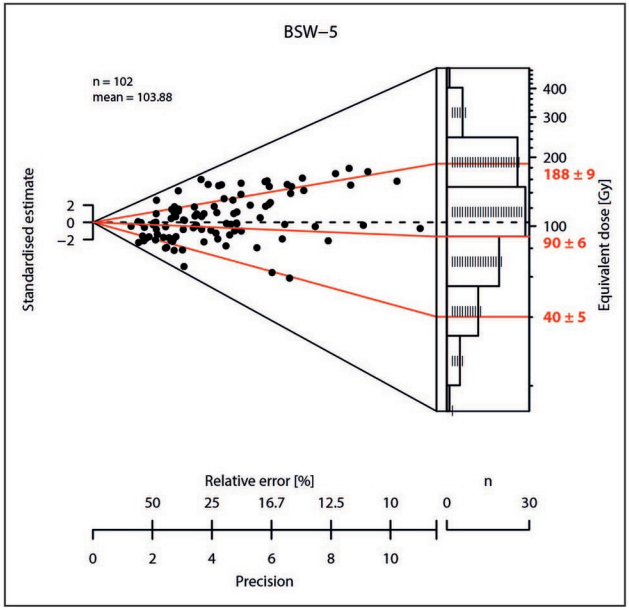
BSW–5
n = 102
mean = 103.88
Standardised estimate
Equivalent dose [Gy]
188 ± 9
90 ± 6
40 ± 5
Relative error [%]
n
Precision

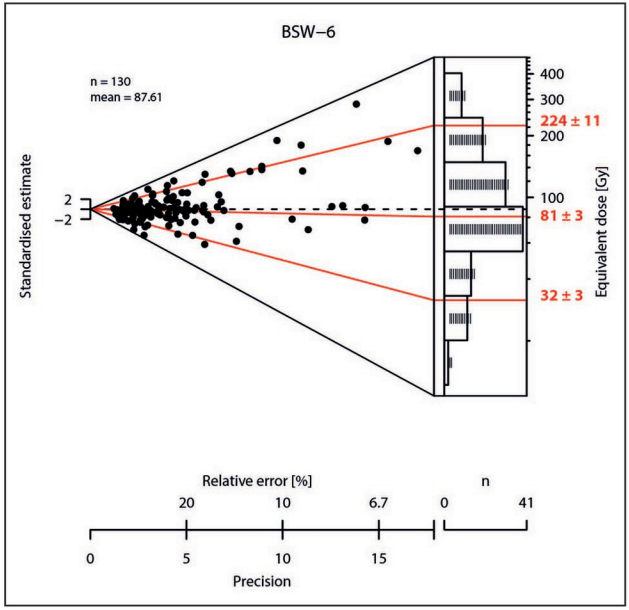
BSW–6
n = 130
mean = 87.61
Standardised estimate
Equivalent dose [Gy]
224 ± 11
81 ± 3
32 ± 3
Relative error [%]
n
Precision

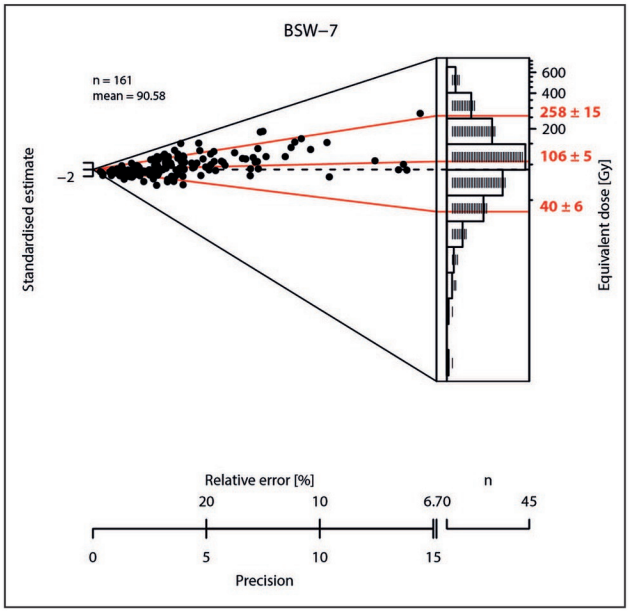
BSW–7
n = 161
mean = 90.58
Standardised estimate
Equivalent dose [Gy]
258 ± 15
106 ± 5
40 ± 6
Relative error [%]
n
Precision

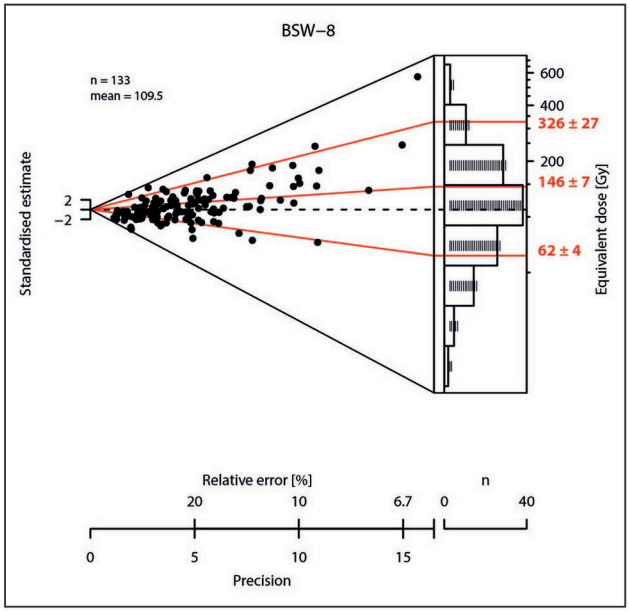
BSW–8
n = 133
mean = 109.5
Standardised estimate
Equivalent dose [Gy]
326 ± 27
146 ± 7
62 ± 4
Relative error [%]
n
Precision

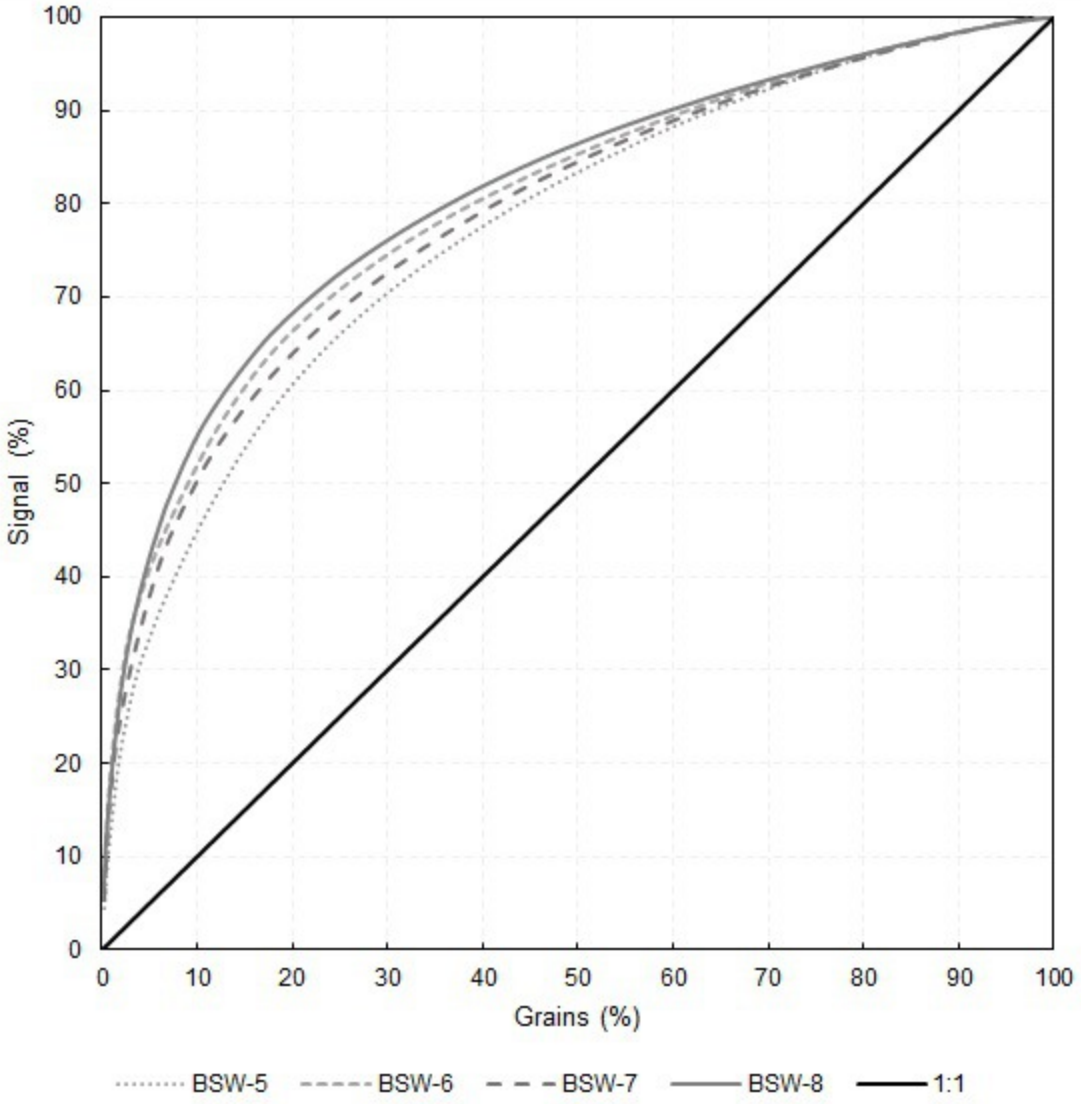
100
90
80
70
60
50
40
30
20
10
0
Signal (%)
0
10
20
30
40
50
60
70
80
90
100
Grains (%)
BSW-5
BSW-6
BSW-7
BSW-8
1:1

Tables

Step	Treatment
1	Give a regenerative dose (for N, dose = 0)
2	Preheat at 260°C for 10 s
3	Blue LED stimulation at 125°C for 300 s
4	Preheat at 260°C for 10 s
5 ($L_{TT\text{-}OSL}$)	SG Green laser stimulation at 125°C for 2 s
6	Give a test dose of ~25 Gy
7	Preheat at 220°C for 5 s
8 (T_{OSL})	SG Green laser stimulation at 125°C for 2 s
9	Deplete remaining signal with blue stimulation at 310°C for 100 s
10	Return to 1

Tab. 1. TT-OSL SAR measurement protocol applied to single grain (SG) quartz. Shaded steps were used to construct the dose response curve.

Sample	Burial depth (cm)	n/N	Yield (%)	Total dose rate (Gy/ka)	D_e (Gy)	Age (ka)
BSW-5	192	102/500	20	0.83 ± 0.02	188 ± 9	**226 ± 13**
BSW-6	215	130/1000	13	0.76 ± 0.02	224 ± 11	**295 ± 17**
BSW-7	218	161/1100	15	0.74 ± 0.02	258 ± 15	**350 ± 22**
BSW-8	233	133/1100	12	0.89 ± 0.03	326 ± 27	**366 ± 32**

Tab. 2. Single grain TT-OSL ages obtained for Bestwood 1. The De were measured using the standard 300 µm holes-disk, with 3-4 grains in each hole. Ages were calculated using the oldest component obtained from the Finite Mixture Model (SOM Tab. S3). Alpha, beta and gamma dose rates were calculated from the radioactive elements measured by ICP-MS (U, Th) and ICP-OES (K) and are provided in SOM Tab. S1. Cosmic dose rates were estimated from current burial depths (see text).